Observational Evidence for Asymmetric Changes in Tropospheric Heights over Antarctica on Decadal Time Scales

W. Neff [1], J. Perlwitz [1,2], & M . Hoerling [1]
[1] NOAA/Earth System Research Laboratory, Boulder Colorado, 80305
[2] Cooperative Institute for Research in the Environmental Sciences, University of Colorado, Boulder, Colorado, 80305

Abstract

We use monthly values of geopotential height (GPH) from seven Antarctic stations to examine decadal variations and trends in the overlying troposphere. Whereas the stratospheric signal in our analyses associated with springtime ozone depletion is very detectable, documenting changes in the troposphere is complicated by strong decadal variability and geographical asymmetry. On the Indian-Ocean coast of Antarctica, negative trends in 500-hPa GPH prevail from December through May but lower GPH following extreme depletion episodes is only found from December through February. In contrast, the South Pole, McMurdo, and Halley Stations show positive trends for most months and heights with no depletion signal evident in GPH at the South Pole and Halley Stations except at and above 100 hPa. These observed seasonal and geographical asymmetries suggest that the internal dynamical response in the troposphere over Antarctica to climate change and ozone depletion is more complex than is captured in current models.

1. Introduction

The Antarctic Oscillation, also referred to as the Southern Hemisphere Annular Mode (SAM), has been described as an exchange of mass between mid- and high-latitudes that is equivalent barotropic in structure with manifestations both in surface pressure fields [*Gong and Wang*, 1999] and in the strength of the circumpolar circulation in both the troposphere and stratosphere [*Thompson and Wallace*, 2000]. A trend in the observed SAM toward its positive phase in the 1980s and 1990s has been attributed to stratospheric ozone depletion in the austral spring [*Thompson and Solomon*, 2002] combined with the influence of increasing greenhouse gases (GHG) [*Arblaster and Meehl*, 2006; *Marshall et al.*, 2004; *Shindell and Schmidt*, 2004]. Some results in the literature have suggested that the increase in the SAM is also manifested as a cooling of the surface over east Antarctica, particularly from 1969 to 1998 [*Thompson and Solomon*, 2002]. Others have raised the issue of the relative roles of anthropogenic forcing and multidecadal variability on recent surface temperature trends [*Monaghan et al.*, 2008a] and pointed out pointed out limitations in current models in their ability to reproduce observed temperature trends over Antarctica [*Monaghan et al.*, 2008b]. Meanwhile, additional factors have been implicated in Antarctic circulation changes such as the increase in circumpolar westerlies in autumn due to changes in the semi-annual oscillation (SAO) [*Bracegirdle et al.*, 2008] and an increase in zonal wave one after 1975 which was also associated with an increased tendency for ridging in the southeast Pacific [*Raphael*, 2003]. The origin of a wave-one field may also lie in lower latitudes such as from the Indian Ocean [*Quintanar and Mechoso*, 1995]. An analysis of 300-hPa GPH anomalies [*Neff*, 1999: Figure 13] showed that increased October cloudiness at the South Pole was associated with a GPH anomaly pattern similar to that now associated with the high index state of the SAM (http://www.cpc.ncep.noaa.gov) whereas low-cloud-fraction conditions occurred with a wave-one pattern that favored 300-hPa wind directions associated with lighter surface winds and colder temperatures. A better definition of anomaly patterns such those due to the SAM and/or wave-one are thus important to diagnosing temperature trends over Antarctica, particularly in light of results linking winds aloft to surface temperatures over the interior of the continent [*Neff*, 1999].

Unfortunately, numerical simulations and observations have not produced consistent results for the predicted tropospheric signal due to ozone depletion over Antarctica. For example, while *Thompson and Solomon* [2002] found significant negative trends from 1969 to 1998 in observed GPH at 500 hPa, primarily from stations along east Antarctica, during December and January and again during April and May, the latter changes in autumn were not found in the numerical simulations of *Gillett and Thompson* [2003]. More recent simulations of GPH on the eastern rim of Antarctica [*Arblaster and Meehl*, 2006] did not show significant negative trends in the troposphere below 300 hPa (their Figure 3) arising from ozone depletion in either period although they did find significant DJFMAM trends in sea level pressure and surface temperature in reasonable agreement with ERA-40 results. Meanwhile, others [*Crook et al.*, 2008] have argued that an increasing asymmetry in the stratospheric ozone distribution may have accentuated recent trends in GPH and temperature, particularly those associated with quasistationary planetary waves [*Grytsai et al.*, 2007].

Such results suggested further exploration of the potential for asymmetric and multidecadal-changes in the lower troposphere that would affect trend detection. Unfortunately, trend-detection issues remain difficult to resolve empirically because the observational network over

Antarctica is sparse and biased toward the Eastern Hemisphere with the preponderance of surface and upper-air sounding stations located on the coast of Antarctica facing the Indian Ocean (Figure 1). It should also be noted that these stations lie on the edge of the east Antarctic ice plateau that is largely offset into the Eastern Hemisphere (see Figure 1). *Marshall* [2003] noted this limitation in the surface network that he used to estimate SAM indices from the zonal mean surface pressure difference between 40^{o}S and 65^{o}S. This paucity of data motivated a closer look at GPH changes over the Antarctic continent that also included data from Amundsen-Scott South Pole and McMurdo Stations as well as those from coastal sites and over the full range of data available from 1957 to the present. Data records from the seven stations used here extend from the late 1950s to the present, as summarized in the Auxiliary Material (Table S1). These data allow a comparison of seasonal trends from stations representing "west" Antarctica (Halley, South Pole, and McMurdo) with trends observed in the Eastern Hemisphere (Mawson, Davis, Mirny, and Casey). This comparison is of particular interest because winter extremes in the SAM (measured by the coast-to-midlatitude surface pressure difference) have been found to coincide with changes in cyclone density and depth along the east coast of Antarctica determined from reanalyses [*Pezza et al.*, 2008]. Because the South Pole is fairly isolated from coastal weather effects [*Neff*, 1999], it should allow a distinction between trends due to changes in the mid-to-high latitude storm track and those evident near the center of the polar vortex. We have also used observations of total ozone column in November (TOC, http://www.esrl.noaa.gov/gmd/) at the South Pole from 1961 through 2007 to contrast changes in GPH at coastal sites with those observed over the interior of the continent in the months following major springtime ozone depletion episodes.

2. Data

Figure 1 showed the upper-air stations used in the current analysis and Table S1, the durations of their records. The primary source for these data has been the READER project [*Turner et al.*, 2004]. Where gaps existed in these data, they have been filled to the extent possible by reexamination of actual sounding data as well as GPH published as monthly averages in the Climate Data Volumes of the former U.S. Weather Bureau. The latter data have been useful, particularly at the South Pole where the original sounding data were not preserved for the period prior to 1961. Because of reasonable correlation between adjacent stations from Mawson extending east to Casey (Table S2), we have averaged these data together to form a Mawson-to-

Casey Composite (MCC) so as to examine trends along this sector of coastal eastern Antarctica. In comparing GPH interannual variability at South Pole with Halley and McMurdo, we found significance covariance but with a systematic decrease in average GPH from Halley to the South Pole to McMurdo (Table S2). Because these three stations lie in geographically unique locations, we will examine their trends individually. Additional time series were created by combining more intermittent data from stations in close proximity such as Neumayer/Novolazarevskya/SANAE (NNS) and Molodeznaja/Syowa (MS).

Analyses of trends in GPH and 300-hPa winds at the South Pole [*Neff*, 1999] revealed strong variability at 2-to-3 year time scales. This variability was superimposed on a decadal-varying, long-term positive winter trend in the 650-300 hPa thickness from 1961 to 1998, consistent with the continent-wide tropospheric warming reported by *Turner et al.* [2006]. To address the interannual variability we examined the power spectral density of detrended time series of monthly averaged 500-hPa GPH for several months with and without strong trends. These typically reveal a spectral gap at periods of about four-years (Figure S1) although time series dominated by strong trends reveal lower levels of interannual-to-decadal variability. Although this gap is not present at all sites for all seasons, for consistency we have chosen to use two passes of a five-year triangular filter to reduce inter-annual variability while looking for long-term trends. At the endpoints, the filter was reduced to a three-point and then two-point average, a very simplified method compared to the approach suggested by *Mann* [2004]. This approach minimizes the effect of endpoint extremes (see Figure S2 for an example).

3. Analysis of Trends

Figure 2 shows the results of our analysis of 500-hPa GPH trends and of GPH data stratified by high and low total ozone column (TOC) in November recorded at the South Pole. The use of these data was motivated by the extensive analysis of *Neff* [1999] who argued that sounding data from the South Pole, located within the polar vortex, provided an accurate view of the evolution of the ozone hole when compared with satellite data. Figures 2a,b,c provide smoothed GPH time series for September, December and May, respectively, for MCC and SP with the Marshall Index (http://www.antarctica.ac.uk/met/gjma/sam.html) shown for comparison (after inverting and matching to the mean and variance of the 500 hPa GPH time series for MCC). Given that the Marshall Index is derived from surface station pressure differences between the coast and mid-latitudes, the agreement with coastal 500-hPa GPH in the Eastern Hemisphere is quite good.

For the presentation here, September was chosen because past work showed it to have a nearly zero trend whereas December and May showed maximum negative trends at 500 hPa [*Thompson and Solomon*, 2002]. In our extended time series, September shows a strong and nearly linear positive trend in GPH at the SP, standing in marked contrast to the minimal trend in MCC obtained along the Indian Ocean coast of the continent. Both the December and May time series show much stronger decadal variability, with distinct minima in the early 1960s and again in the 1990s, the former consistent with the *Jones and Widmann* [2004] SAM index calculated for December-January.

Figure 2d shows TOC for November at the South Pole which reveals the strong interannual variability in magnitude of ozone depletion and lifetime of the springtime polar stratospheric vortex. Of note is the beginning of significant decreases in November TOC in 1980 followed by strong variability over two-to-six year time scales. A series of extreme depletion events that began in 1987 are identified in the figure: we stratified the GPH data by these values of the November TOC smaller than 203 Dobson Units (DU) and those greater than 300 DU for each month from November through the following May for the interior Antarctic site, SP (Figure 2e) and the east Antarctic sites, MCC (Figure 2f). Comparing these two figures shows a strong coastal signature of low GPH in low-ozone years, for the months of December through February, contrasted with a simultaneous absence of a signature at the SP located on the high plateau. We pursued this result further, examining time series from Halley and McMurdo Stations, relaxing the constraint on stratifying the data to cases with the November TOC < 253 DU and TOC > 300 DU to increase the number of samples in the averages (Figure S3). We found that that McMurdo shows a result similar to but slightly smaller than that from MCC while Halley mirrors results from SP, showing no significant lowering of GPH in low-ozone years.

We also examined (Figure S4) the distribution of monthly GPH values from each of these four time series for the 52 years from 1957 through 2008, during January, the month in which the difference in GPH between low- and high-ozone years peaks. These raw time series reveal interesting changes in these populations on decadal time scales: 1) for the South Pole, the distribution is fairly uniform except for a clustering of low GPH values in the early 1960s, 2) on the east coast of Antarctic (MCC), there is systematically lower GPH starting in 1990 (for both higher and lower TOC values) with a short period of lower GPH in the early 1960s similar to that at SP, 3) at Halley the decadal changes in GPH populations are unremarkable, and 4) at McMurdo, there are generally lower values of GPH in the early 1960s and 1990s (alternatively, one might view the period from 1965 to 1990 as "abnormal" with contrasting larger values of GPH). This latter result highlights the difficulty of deducing trends from even five decades of data from the Antarctic: Such results also argue for independent measures of the SAM index such as the work of *Jones and Widmann* [2003].

Figure 2g summarizes the linear trend analysis on a monthly basis for MCC and SP with 95% confidence intervals indicated. The linear trends for MCC are most robust and negative during the fall whereas at SP, they are most robust and positive in the spring. Interestingly, the month-to-month changes in the trends from the two series track each other closely on an annual basis, especially from March through December, with an average positive offset of about 1.2 m/yr at SP compared to MCC. Because the SP and MCC time series analyses show distinct seasonal effects in their trends, we examined their trends compared to other coastal sites as well as with the more limited record from Vostok Station (as summarized in Figures S5 and S6 and attendant discussion, which show substantial agreement with the trends at the South Pole). The other coastal sites included McMurdo and Halley Bay (see Figure 1), as well as the series of stations on the "northern" coast of Antarctica from 8^{o}W to 46^{o}E that we blended into the two composite time series NSS and MS. In Figure 2h we have plotted these trends for September, December, and May (summarized in Table S3 and shown graphically in Figure S7) moving counterclock-wise around the continent for each of our six time series starting with the east coast time series, MCC. This figure reveals the systematic geographical asymmetry in trends common to these three months, with positive increments in the trends, moving counterclockwise from the Eastern Hemisphere to the Western Hemisphere. This behavior is largely independent of season as seen for these three months. Taken together, these figures show an annual cycle in GPH trends that is continent wide (Figure 2g) coupled with a systematic negative offset in trends on the east coast of Antarctica compared with those observed in the Western Hemisphere (Figure 2h).

A remaining question is whether the observed behavior of 500-hPa GPH is reflected at higher levels in the Antarctic atmosphere. To examine this question, we calculated trends at 300, 200, 100, and 50 hPa for Halley, South Pole, McMurdo, and East Antarctic stations using READER data as shown in Figure 3. At and above 100 hPa at the South Pole and McMurdo, significant gaps in the data occur from the mid-1970s until the late 1980s during the winter (June through September: Figure S8). Because of the data gaps, we calculated linear regression trends only from the raw monthly data. Despite limitations in data availability above 100 hPa in winter and, in some cases, limited statistical significance, these results paint a consistent picture from level to level and from station to station of rising GPH over west Antarctic sites -- except at and above 100 hPa for the period of rapid ozone depletion in the austral spring. Over the east Antarctica coast, year-round negative trends prevail and accelerate during and following the spring ozone depletion period. It should be noted that the trends generally increase in amplitude with height in the atmosphere consistent with decreasing atmospheric density.

4. Summary and Discussion

We have examined changes in 500-hPa geopotential height from seven sounding sites located on the continent of Antarctica, south of 65^{o}S, distributed primarily along the East Antarctic coastline facing the Indian Ocean but included Halley, South Pole, and McMurdo Stations which are on the side of the continent influenced primarily by the Pacific and Atlantic Oceans. Linear least-squares analysis of these time series from 1957 through the present revealed a significant asymmetry in the trend in GPH over the continent. Generally falling GPH from East Antarctic stations was found from December through May (peaking in May) with rising GPH over West Antarctica primarily during the months of May through December (peaking in September). Coincidently, both MCC and SP show the same positive increments in their trends in the winter from May through September, perhaps implying a role for increasing GHG (c.f. Turner et al., [2006]). We examined both the annual cycle of 500-hPa GPH changes as well as their systematic variation around the continental topography, the major portion of which is located off-axis in the Eastern Hemisphere. This suggested the presence of both an annual cycle in GPH trends that is continent wide together with an asymmetric component favoring lower GPH on the Indian Ocean side of the continent, particularly in the fall. Stratifying GPH data by the total ozone column over the interior of Antarctic shed additional light on the changes in GPH following extreme ozone depletion: namely, that a change is observed only in coastal areas, it favors the Indian Ocean side of the continent, and is confined to the months of December through February. However, long-term negative trends observed along the Indian-Ocean coast line of Antarctica extend later and peak in May. Such a result argues that the ozone depletion signal in the troposphere is not axisymmetric over the continent and that other internal dynamical mechanisms must be at play in the troposphere. For example, other dynamical factors complicating the interpretation of long-term changes in the SAM from the limited sounding system in Antarctica are potential trends in asymmetric aspects of the circumpolar vortex [*Raphael*, 2003] and potential pole-ward shifts of storm tracks in a warming climate [*Yin*, 2005]. Furthermore, our analysis can not eliminate the possibility that the same meteorological conditions that favor the more extreme ozone depletion events do not also favor lower GPH along coastal Antarctica and hence the apparent behavior of the SAM deduced from tropospheric observations.

Acknowledgements

We appreciate the comments of Dr. Ryan Fogt and the anonymous reviewers who provided a number of useful suggestions.

References

Arblaster, J. M., and G. A. Meehl (2006), Contributions of external forcings to southern annular mode trends, *J. Clim.*, *19*, 2896-2905.

Bracegirdle, T. J., et al. (2008), Antarctic climate change over the twenty first century, *J. Geophys. Res.*, *113*.

Crook, J. A., et al. (2008), Sensitivity of Southern Hemisphere climate to zonal asymmetry in ozone, *Geophys. Res. Lett.*, *35*.

Gillett, N. P., and D. W. J. Thompson (2003), Simulation of recent Southern Hemisphere climate change, *Sci.*, *302*, 273-275.

Gong, D., and S. Wang (1999), Definition of Antarctic oscillation index, *Geophys. Res. Lett.*, *26*, 459-462.

Grytsai, A. V., et al. (2007), Structure and long-term change in the zonal asymmetry in Antarctic total ozone during spring, *Annales Geophysicae*, *25*, 361-374.

Jones, J. M., and M. Widmann (2003), Instrument- and Tree-Ring-Based Estimates of the Antarctic Oscillation, *J. Clim.*, *16*, 3511-3524.

Jones, J. M., and M. Widmann (2004), Atmospheric science - Early peak in Antarctic oscillation index, *Nature*, *432*, 290-291.

Mann, M. E. (2004), On smoothing potentially non-stationary climate time series, *Geophys. Res. Lett.*, *31*.

Marshall, G. J. (2003), Trends in the Southern Annular Mode from Observations and Reanlysis, *J. Clim.*, *16*, 4134-4143.

Marshall, G. J., et al. (2004), Causes of exceptional atmospheric circulation changes in the Southern Hemisphere, *Geophys. Res. Lett.*, *31*.

Monaghan, A. J., et al. (2008a), Recent variability and trends of Antarctic near-surface temperature, *J. Geophys. Res.*, *113*.

Monaghan, A. J., et al. (2008b), Twentieth century Antarctic air temperature and snowfall simulations by IPCC climate models, *Geophys. Res. Lett.*, *35*.

Neff, W. D. (1999), Decadal time scale trends and variability in the tropospheric circulation over the South Pole, *J. Geophys. Res.*, *104*, 27217-27251.

Pezza, A. B., et al. (2008), Southern hemisphere synoptic behavior in extreme phases of SAM, ENSO, sea ice extent and Southern Australia rainfall, *J. Clim*, In Press.

Quintanar, A. I., and C. R. Mechoso (1995), Quasi-stationary waves in the Southern Hemisphere. Part I: Observational data, *J. Clim.*, *8*, 2659-2672.

Raphael, M. (2003), Recent, large-scale changes in the extratropical southern hemisphere atmospheric circulation, *J. Clim.*, *16*, 2915-2924.

Shindell, D. T., and G. A. Schmidt (2004), Southern Hemisphere climate response to ozone changes and greenhouse gas increases, *Geophys. Res. Lett.*, *31*.

Thompson, D. W. J., and S. Solomon (2002), Interpretation of Recent Southern Hemisphere Climate Change, *Sci.*, *296*, 895-899.

Thompson, D. W. J., and J. M. Wallace (2000), Annular Modes in the Extratropical Circulation. Part I: Month-to-Month Variability, *J. Clim.*, *13*, 1000-1016.

Turner, J., et al. (2004), The SCAR READER project: Toward a high-quality database of mean Antarctic meteorological observations, *J.Clim.*, *17*, 2890-2898.

Turner, J., et al. (2006), Significant warming of the Antarctic winter troposphere, *Sci.*, *311*, 1914-1917.

Yin, J. H. (2005), A consistent poleward shift of the storm tracks in simulations of 21st century climate, *Geophys. Res. Lett.*, *32*.

Figure Captions

Figure 1. Antarctic topography with locations of long-term sounding stations. Sites with nearly complete records from 1957 to the present are shown in red whereas those stations that were grouped to provide long records or have shorter duration are shown in blue. At the South Pole, "north" is defined to lie along the Greenwich (or Prime) Meridian. Note that the majority of high terrain of the continent lies off-axis in the Eastern Hemisphere.

Figure 2. (a,b,c) Variation in GPH for the South Pole (SP: solid circles) and East Antarctica (MCC: Open Diamonds) for the months indicated, together with the Marshall SAM Index, inverted and adjusted to the mean and standard deviation of the MCC time series (red line), (d) Total November ozone column at the South Pole for 1961-2007: solid blue diamonds indicate low-ozone events, (e) Average GPH at SP for low ozone (<200 DU, blue) and high ozone (>300 DU, red): shading shows standard error of estimate, (f) same as (e) for MCC, (g) trends and 95% confidence intervals for 500-hPa height trends on a monthly basis for the South Pole (solid circles) and MCC (open diamonds), (h) systematic change in GPH trends for September (solid circles), December (solid squares), and May (solid diamonds) taken in a counter-clockwise sense from East Antarctica (MCC) to McMurdo Station (MCM) derived from Table S3.

Figure 3. Monthly trends at 500 (Yellow), 300 (Orange), 200 (Red), 100 (Gray) and 50 (Black) hPa on a monthly basis from 1957 to the present from seven Antarctic sounding stations: (a) MCC, (b) Halley, (c), South Pole, and (d) McMurdo. Gaps occur either with cases of zero trend or with major data gaps that made trend detection impossible.

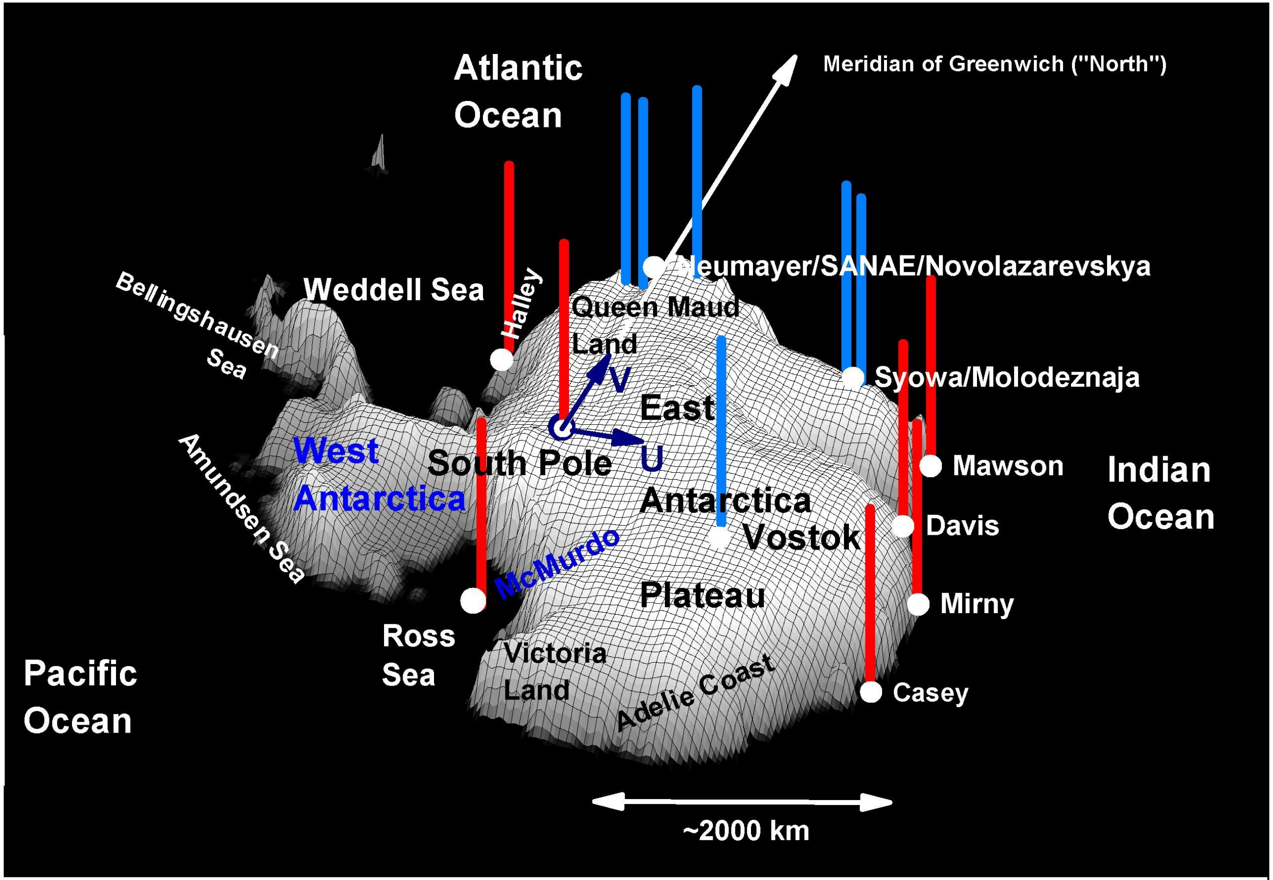

Atlantic Ocean
Meridian of Greenwich ("North")
Weddell Sea
Bellingshausen Sea
Halley
Neumayer/SANAE/Novolazarevskya
Queen Maud Land
V
Syowa/Molodeznaja
East
West Antarctica
South Pole
U
Mawson
Indian Ocean
Amundsen Sea
Antarctica
Davis
Vostok
McMurdo
Plateau
Mirny
Ross Sea
Victoria Land
Pacific Ocean
Adelie Coast
Casey
~2000 km

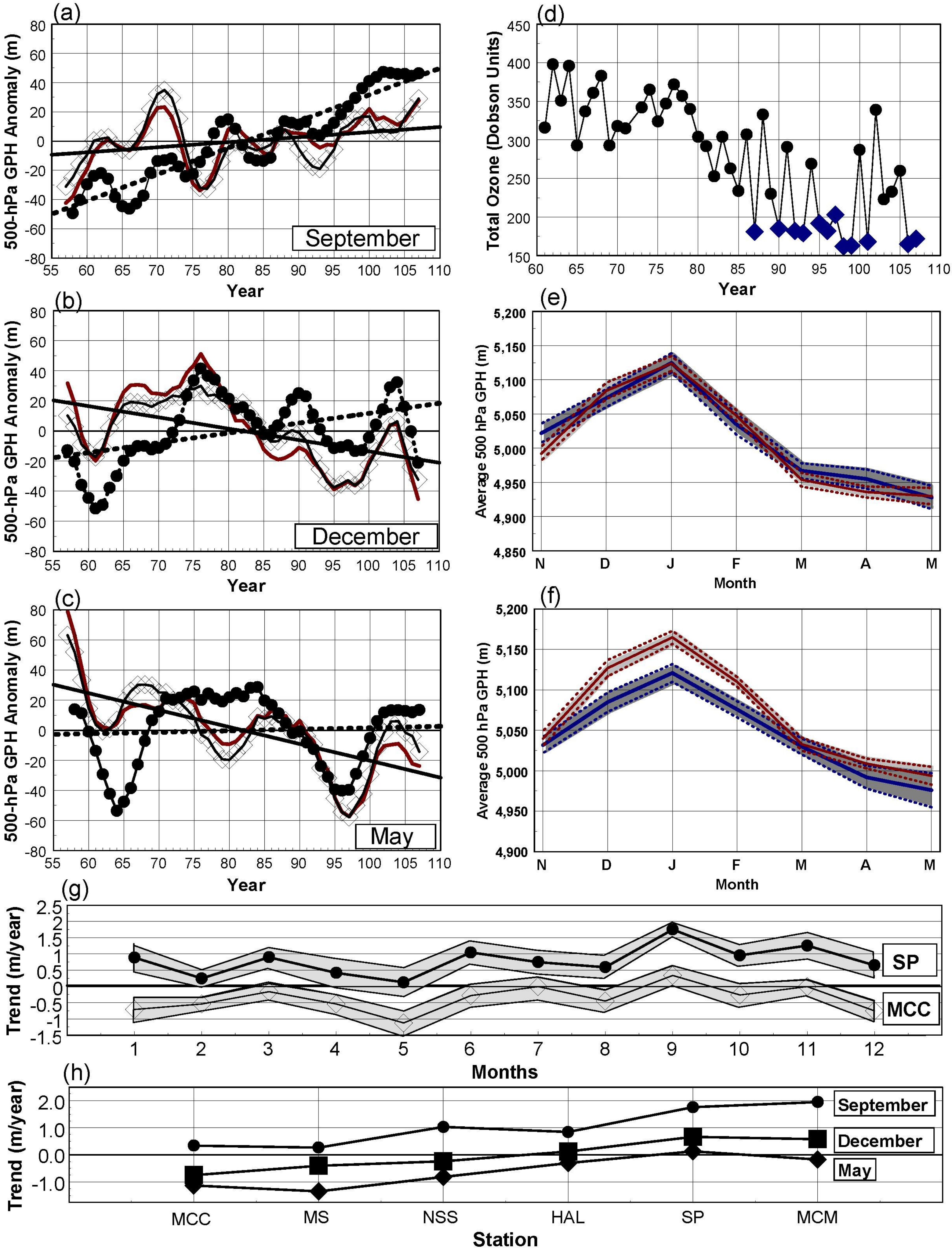

(a)
500-hPa GPH Anomaly (m)
September
Year
(b)
December
(c)
May
(d)
Total Ozone (Dobson Units)
(e)
Average 500 hPa GPH (m)
Month
N D J F M A M
(f)
(g)
Trend (m/year)
SP
MCC
Months
(h)
September
December
May
MCC MS NSS HAL SP MCM
Station

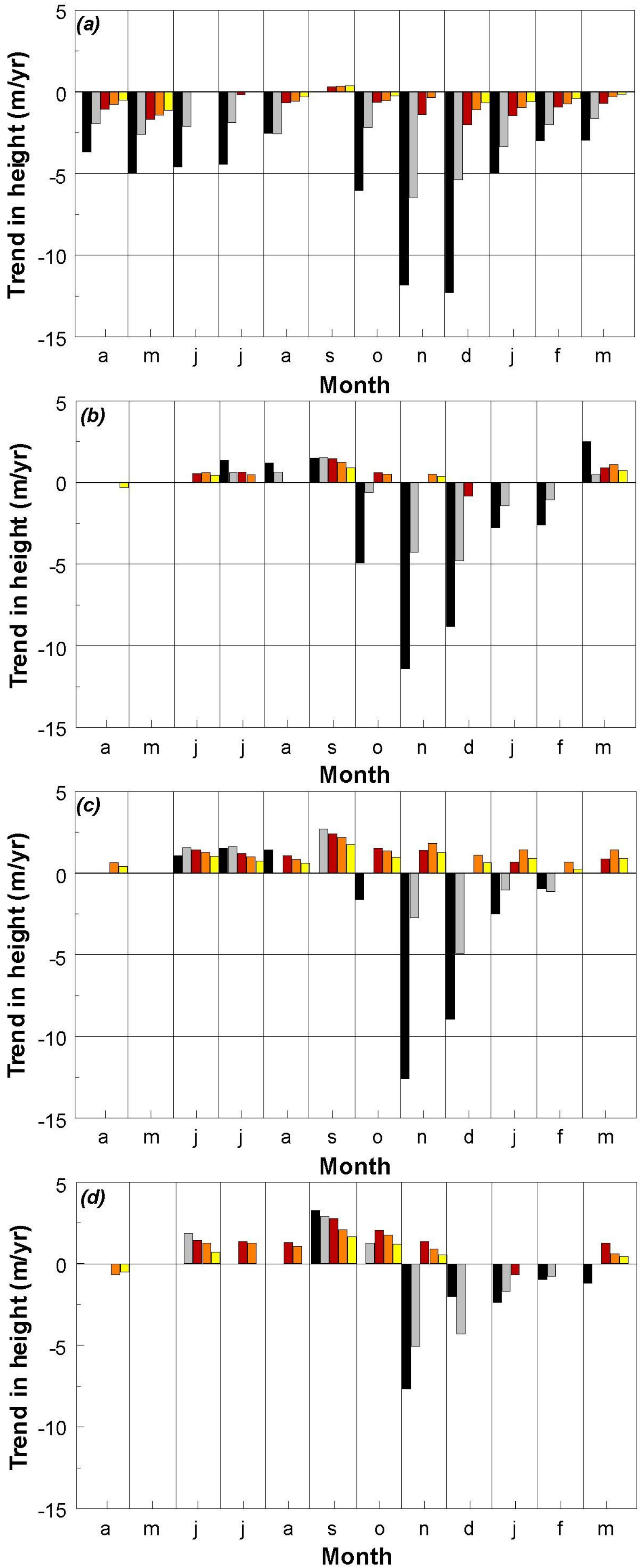

(a)
5
0
-5
-10
-15
Trend in height (m/yr)
a m j j a s o n d j f m
Month
(b)
5
0
-5
-10
-15
Trend in height (m/yr)
a m j j a s o n d j f m
Month
(c)
5
0
-5
-10
-15
Trend in height (m/yr)
a m j j a s o n d j f m
Month
(d)
5
0
-5
-10
-15
Trend in height (m/yr)
a m j j a s o n d j f m
Month